

Statistical Modelling of Fracture in the Ductile-to-Brittle Transition Region

REFERENCE Wallin, K., *Statistical modelling of fracture in the ductile-to-brittle transition region*, *Defect Assessment in Components – Fundamentals and Applications*, ESIS/EGF9 (Edited by J. G. Blauel and K.-H. Schwalbe) 1991, Mechanical Engineering Publications, London, pp. 415–445.

ABSTRACT Statistical modelling of cleavage fracture initiation has become increasingly popular during the last few years. Several different models, for describing the behaviour of fracture toughness in the cleavage fracture temperature region, have been presented. Even though the models may differ considerably in their basic assumptions of the microscopic fracture mechanism, macroscopically most of them still yield an identical result.

When considering the ductile–brittle fracture transition region the case is more complex and therefore the number of models describing it is not so large. In this region the fracture initiation is affected by large-scale yielding effects as well as the effect of ductile tearing prior to cleavage fracture initiation. This increased complexity is also reflected upon the existing models as to yield macroscopically different results.

In this paper different existing models for cleavage fracture initiation are examined and a general model is derived in order to explain why the different models yield an identical macroscopic result. Furthermore, also the differences in models describing the ductile-to-brittle transition region are explained and finally an alternative simple correction function for fracture toughness results in the ductile-to-brittle transition region is presented and verified.

Introduction

The different possible mechanisms of cleavage fracture initiation are rather well known. It has been recognised that the critical steps for cleavage fracture are (1):

- (I) initiation of a microcrack e.g. fracturing of a second phase particle;
- (II) propagation of this microcrack into the surrounding grains;
- (III) further propagation of the propagating microcrack into other adjacent grains.

Depending on temperature, loading rate, and material, different steps are more likely to be most critical. Because materials generally are not uniform on a microscale, cleavage fracture initiation has a statistical nature. Attempts to describe this statistical nature have been made since the presentation of the Ritchie, Knott, and Rice model (2). The first attempt to develop a quantitative statistical model for cleavage fracture initiation was carried out by Curry and Knott in 1979 (3).

The need for statistical modelling of cleavage fracture initiation has been acknowledged during the last few years. A number of models, for describing the behaviour of fracture toughness in the cleavage fracture temperature region, have been presented. Most of them are based on the assumption of

* Technical Research Centre of Finland (VTT), Metals Laboratory, Finland.

cleavage fracture initiation to behave like weakest link statistics i.e. one single critical event is sufficient to cause macroscopic failure. Even though the models may differ quite a lot in their basic assumptions of the microscopic fracture mechanism, macroscopically they still yield similar results.

In the ductile–brittle fracture transition region, the cleavage fracture initiation is more complex. In this region the fracture initiation is affected by large-scale yielding effects as well as the effect of ductile tearing prior to cleavage fracture initiation. Some attempts have been made to develop statistical models to also describe this temperature region. Here the increased complexity is reflected upon the existing models as to yield macroscopically different results.

In this paper different existing models for cleavage fracture initiation are examined and a general model is derived in order to explain why the different models yield similar macroscopic results. Furthermore also the basic differences in the models describing the ductile-to-brittle transition region are evaluated and finally an alternative simple correction function for fracture toughness results in the ductile-to-brittle transition region is presented and verified.

General statistical model for cleavage fracture initiation

The basis of the statistical model is presented in Fig. 1. It is assumed that the material in front of the crack contains a distribution of possible cleavage fracture initiation sites, i.e., cleavage initiators. The cumulative probability distribution for a single initiator being critical can be expressed as $P(a \geq a_c)$ and it is a complex function of the initiator size distribution, stress, strain, grain size, temperature, stress, and strain rate etc. The shape and origin of the initi-

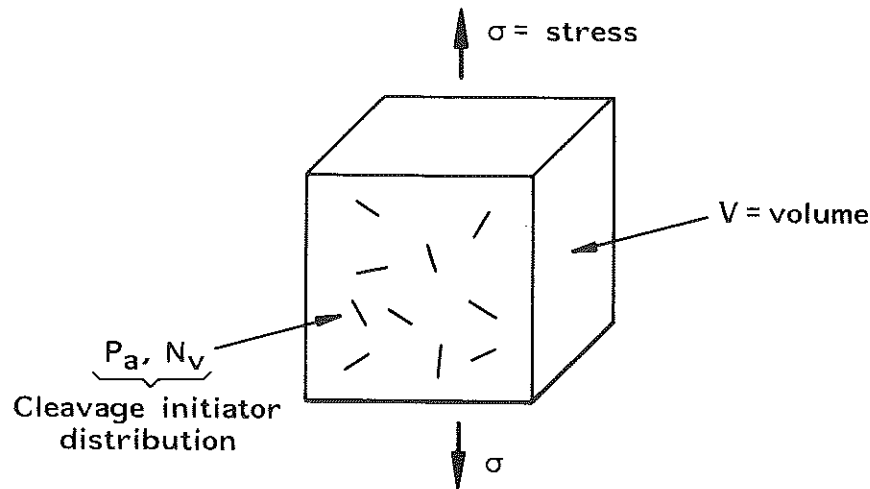


Fig 1 Basis of the general statistical model

ator distribution is not important in the case of a 'sharp' crack. The only necessary assumption is no global interaction between initiators. This means that interactions on a local scale are permitted. Thus a cluster of cleavage initiations may be required for macroscopic initiation. In such a case the cluster forms the critical initiator and it can be treated as a single event. Also the assumption does not cause any restrictions on whether initiation or propagation is most critical. All the above factors can be implemented into the initiator distribution and they are not significant as long as no attempt is made to determine the shape of the distribution.

The cumulative failure probability of a volume element, with an uniform stress state, can be expressed as

$$P_f = 1 - \{1 - P(a \geq a_c)\}^{N_v \cdot V} \quad (1)$$

where N_v is the number of initiators in unit volume and V is the volume of the element.

Equation (1) can also be re-written as

$$P_f = 1 - \exp [V \cdot \ln \{1 - P(a \geq a_c)\}^{N_v}] \quad (2)$$

In the case of several independent homogeneous volume elements, with size V_i having different states of stress the total cumulative failure probability becomes

$$P_f = 1 - \exp \sum_{i=1}^n V_i \cdot \ln \{1 - P_i(a \geq a_{ci})\}^{N_v} \quad (3)$$

where n is the number of volume elements.

Equation (3) contains one restricting assumption, i.e., that the volume elements are homogeneous so that the number of initiators in a volume element is defined as $N = N_v \cdot V$. In reality the initiators are randomly distributed, which causes N to be not constant, but Poisson distributed (4). If we mark the mean number of initiators with \bar{N} , the probability P_N of having N initiators in a volume element is

$$P_N = \frac{\bar{N}^N \cdot \exp(-\bar{N})}{N!} \quad (4)$$

The probability of initiation in one volume element becomes

$$P_f = 1 - \sum_{N=0}^{\infty} \{1 - P(a \geq a_c)\}^N \cdot P_N \quad (5)$$

Performing the summation one obtains

$$P_f = 1 - \exp [\bar{N} \cdot \{1 - P(a \geq a_c)\}] \cdot \exp(-\bar{N}) \quad (6)$$

which reduces to

$$P_f = 1 - \exp \{-\bar{N} \cdot P(a \geq a_c)\} \quad (7)$$

Thus the form of equation (3), when assuming randomly distributed initiators, is

$$P_f = 1 - \exp \sum_{i=1}^n \{-\bar{N}_v \cdot V_i \cdot P_i(a \geq a_{ci})\} \quad (8)$$

where \bar{N}_v is the mean number of initiators per unit volume.

If the probability of an initiator being critical is smaller than 0.1, equations (3) and (8) are practically identical. Because the probability of an initiator being critical is usually much smaller than 0.1 it is really arbitrary which form to use.

It should be emphasised that the above expressions contain no approximations.

For a 'sharp' crack in small-scale yielding the stresses and strains are described by the HRR field. One property of the HRR field is that the stresses have an angular dependence. Thus the stress field can be divided into small fan-like elements with an angle increment $\Delta\theta$. In this case the cumulative failure probability becomes

$$P_f = 1 - \exp \sum_{\theta=0}^{2\pi} \left\{ \sum_{x=0}^{x_p} -\bar{N}_v \cdot B \cdot \Delta x \cdot x \cdot \sin(\Delta\theta) \cdot P(a \geq a_c) \right\} \quad (9)$$

where the volume element in the x direction, described by Δx must be clearly larger than the initiator size a . The double summation indicates that the summation is performed over the whole plastic zone.

Due to the properties of the HRR field it is possible to normalise the distance with the stress intensity factor

$$U = \frac{x}{(K_I/\sigma_y)^2} \quad (10)$$

When equation (10) is inserted into equation (9) the cumulative failure probability becomes

$$P_f = 1 - \exp \left[B \cdot \sin(\Delta\theta) \cdot \frac{K_I^4}{\sigma_y^4} \cdot \sum_{\theta=0}^{2\pi} \left\{ \sum_{U=0}^{U_p} -\bar{N}_v \cdot U \cdot \Delta U \cdot P(a \geq a_c) \right\} \right] \quad (11)$$

The result of the double summation is always negative and independent of K_I . This enables us to write

$$P_f = 1 - \exp(-\text{const.} \cdot B \cdot K_I^4) \quad (12)$$

It is seen that the scatter of fracture toughness is really independent of the cleavage initiator distribution. The result contains no approximations. The only assumption is that the initiators are independent on a global scale. In other words it is assumed that the volume elements are independent for a

constant K_I . Only, if it is assumed that a certain fraction of the crack front must experience critical initiations to cause macroscopic failure, then the result will differ from equation (12). In the derivation, the cleavage fracture process zone was assumed to be equal to the plastic zone. Equation (12) is, however, not sensitive to the definition of the process zone as long as it is assumed that the process zone size correlates with K_I , CTOD, or J . It is interesting to note that equation (12) is identical to the Weibull distribution function with a fixed value for the shape parameter. The result is not, however, related to Weibull statistics in any way but to assume a weakest link type failure mechanism.

Equation (12) would imply that an infinitesimal K_I value might lead to a finite failure probability. This is not true in reality. For very small K_I values the demand for Δx to be clearly larger than the initiator size is violated. Also, for very small K_I values the stress gradient becomes so steep that even if cleavage fracture can initiate it will almost immediately arrest, thus causing a stable type of fracture. This is an effect often seen with ceramics. Finally, the pre-fatiguing process causes a warm pre-stress effect. All these factors lead to a lower limiting K_{\min} value below which cleavage fracture is impossible. For test specimens of steel it seems that the pre-fatigue load governs the value of K_{\min} . This assumption is based on acoustic emission measurements where it has been found that acoustic emission occurs only at load levels above the pre-fatigue load (5).

Allowing for K_{\min} the equation describing the fracture toughness scatter can be written as

$$P_f = 1 - \exp \left\{ -\frac{B}{B_0} \left(\frac{K_I - K_{\min}}{K_0 - K_{\min}} \right)^4 \right\} \quad (13)$$

In equation (13), B_0 and K_0 are normalisation constants. The normalisation thickness B_0 can be made equal to any desired reference thickness. The scale parameter K_0 corresponds to a 63.2 percent fracture probability, for thickness B_0 , and is approximately given by $K_0 = 1.1 \cdot K_{\text{mean}}$.

Next, other existing statistical cleavage fracture models are compared on the basis of the general model.

Other statistical models for cleavage fracture initiation

During the past years a relatively large number of statistical models for cleavage fracture have been developed. It would be unrealistic to try to describe them all here, but a short chronological review on their evolution will be attempted.

Ritchie, Knott, and Rice (2) were the first to apply statistical considerations to the cleavage fracture initiation event. They concluded that the critical cleavage fracture stress must be achieved over a 'characteristic' distance. Thus they actually defined a critical volume, because of the angular nature of the stress distribution. They did not, however, perform any statistical derivations,

and therefore their model (RKR) cannot be regarded as a true statistical model.

The first attempt to develop a quantitative statistical model for cleavage fracture initiation was performed by Curry and Knott (3). Their model was much more refined than the RKR model. They based their treatment on the actual carbide size distribution and, combining it with a cleavage fracture criterion and the stresses in front of the crack, calculated a probabilistic estimate for K_{IC} . Unfortunately their derivations contain unnecessary approximations that lead to an overly simplified result. Instead of predicting the scatter in fracture toughness, they obtain only one single value. They also assume that fracture nucleation is sympathetic across the crack front, thus predicting no statistical thickness effect. Curry proposed that the RKR model could also be interpreted as a statistical model similar to the Curry and Knott model (6).

Another approach was used by Landes and Shaffer (7). They assumed that the scatter in fracture toughness followed the two parameter Weibull distribution, where the shape parameter was taken as material and temperature dependent. This approach has since been applied by several investigators, for example, Andrews, Kumar, and Little (8), Brückner and Munz (9) and Satoh, Toyoda, and Minami (10). Later Landes and McCabe (11) attempted to improve the method by including a third parameter for the minimum toughness. The disadvantage with this approach is that it lacks a sound theoretical background, and that it contains two-three unknown fitting parameters.

Since these 'first' attempts several new models have been developed. Here, some of them will be presented and compared on the basis of the general model presented above. The micromechanical background of the different models will not be discussed in detail. The models will mainly be examined from a statistical point of view. The main differences in the different models lie in the physical definition of $P(a \geq a_c)$ and the cleavage fracture process zone.

The initial derivation of the macroscopic scatter in cleavage fracture was performed by the Beremin group (12) and first presented by Pineau in 1981 (13). They assume pure weakest link behaviour for cleavage fracture, describe $P(a \geq a_c)$ with a two parameter Weibull distribution function, define the cleavage fracture process zone by the plastic zone size and end up with an equation identical to equation (12). One of the most comprehensive descriptions of the model is by Mudry (14). The Beremin model has become quite widely spread and it has been applied and modified by a number of investigators. Two early applications of the Beremin model were performed by Qu, Wang, and Tsai (15) who tried to determine the parameters experimentally and Hou *et al.* (16) who applied it to describe the notch acuity effect on measured cleavage fracture stress.

Evans (17) developed another model for cleavage fracture. He defines $P(a \geq a_c)$ as

$$P(a \geq a_c) = \left(\frac{\sigma - \sigma_u}{\sigma + \sigma_0} \right)^m \quad (14)$$

Evans divides the crack front into slits and assumes that fracture of each slit is described by weakest link statistics. Thus he obtains an equation like equation (12) for the fracture of a single slit. However, Evans assumes that a certain percentage of slits (50 percent) must be subject to cleavage fracture in order to produce unstable extension of the major crack. Therefore the Evans model is not a true weakest link model. Furthermore, it does not predict any scatter or size effects in the fracture toughness. From a micromechanistic point of view the Evans model would seem to be more suitable for describing ductile tearing than cleavage fracture.

Wallin, Saario, and Törrönen derived a model (WST) based on the actual cleavage fracture micromechanism (18). They derived a theoretical expression for $P(a \geq a_c)$. By further developing the micromechanical assumptions in the Curry and Knott model (3) they assumed the primary cleavage initiators to comprise of brittle second phase particles like carbides. The probability of finding a broken carbide having the radius greater than or equal to r_0 can, according to the model, be expressed as (19)

$$P^*(r \geq r_0) = \int_{r_0}^{\infty} P_{fr} \cdot P\{r_0\} \cdot \partial r \quad (15)$$

where $P\{r_0\}$ is the carbide size distribution and P_{fr} is the probability of a carbide fracturing. It was shown that the particle size distribution is well described by (20)

$$P\{r_0\} = \frac{(\vartheta - 2)^{\vartheta-1}}{\Gamma(\vartheta - 1)} \cdot \left(\frac{r_0}{\bar{r}} \right)^{-\vartheta} \cdot \exp \left(- \frac{\vartheta - 2}{r_0/\bar{r}} \right) \quad (16)$$

where \bar{r} is the mean particle radius and ϑ is a distribution dependent constant ($\vartheta > 2$).

The probability of a carbide fracturing was described by a statistical model based on the fibre loading model combined with weakest link fracture theory (20). The resulting equation has the form of a Weibull distribution function including the particle size.

$$P_{fr} = 1 - \exp \left[- \left(\frac{r_0}{r_n} \right)^3 \cdot \left(\frac{\sigma}{\sigma_0} \right)^m \right] \quad (17)$$

Equations (16) and (17) have been shown to yield a quantitative description of the fracture behaviour of brittle particles in a ductile matrix (20).

The WST model is capable of explaining quantitatively most of the experimental findings regarding cleavage fracture initiation, e.g., it yielded the first explanation for the notch acuity effect on the cleavage fracture stress (21)(22). Unfortunately, even the WST model constitutes in its present form only a

crude approximation of cleavage fracture initiation. The cleavage initiators are often something else than brittle particles and this should somehow be implemented into the model. Also plasticity, orientation, and grain size effects etc. should be accounted for. Despite these weaknesses, however, the model still yields a good description of the macroscopic factors affecting cleavage fracture initiation (19).

Slatcher (23) was the first to present a derivation of the general model. Based on weakest link statistics he obtains an equation like equation (12), but because he applies J instead of K_I , the shape parameter is equal to 2 and not 4. He makes use of the simplification in equation (3), but this does not affect the outcome of the model. He also discusses the model's physical significance. Additionally, he also presents a more quantitative model (similar to the Beremin model) where $P(a \geq a_c)$ is described by a two parameter Weibull distribution function.

Lin, Evans, and Ritchie (24) have modified the Evans model (17). They (LER) now define $P(a \geq a_c)$ with a three parameter Weibull distribution function, instead of the modification proposed by Evans (17). Like Evans, they also divide the crack front into slits. The resulting fracture probability of a single slit is described by the weakest link type equation (12), but they, as Evans, demand a certain fraction of slits to fracture in order to cause macroscopic crack propagation. Thus the LER model does not predict a statistical size effect on fracture toughness. They do however attempt to calculate the scatter of fracture toughness. This is achieved by assuming that a 5 percent fracture probability corresponds to when 5 percent of the slits have fractured and a 95 percent fracture probability corresponds to a situation when 95 percent of the slits have fractured. This assumption unfortunately is erroneous. The way LER formulate their requirement for macroscopic crack propagation means that the failure probability of a single slit does not correlate with the probability for macroscopic crack propagation. Thus the LER model is unfit to describe the fracture toughness scatter. This error also decreases the usefulness of the model for other applications.

Tyson and Marandet (25) tried out several different definitions of $P(a \geq a_c)$ corresponding to different fits to inclusion size distributions. Otherwise their derivation is similar to the Evans (17) model with the exception that they assume a true weakest link behaviour of the crack front fracture probability. They obtained in all cases an equation like equation (12) to describe the scatter in fracture toughness.

Anderson (26) defines $P(a \geq a_c)$ with a three parameter Weibull distribution function and applies a weakest link assumption. In small-scale yielding he defines the cleavage fracture process zone size (active volume) to be partly related to δ^2 and partly to δ (δ = crack tip opening displacement). Because the part of the active volume related to δ^2 is dominating, he ends up with an equation like equation (12). Subsequently Anderson and Stienstra (27) have refined the model by making the calculations over the whole plastic region.

Godse and Gurland (28) have made an attempt to modify the LER (24) model. They also define $P(a \geq a_c)$ with a three parameter Weibull distribution function and demand a certain fraction of the crack front to fracture to obtain macroscopic crack propagation, but contrary to LER they define the cleavage fracture process zone to have a constant width. This causes the model to be two-dimensional in nature, not relating to the angular stress distribution. Analogous to the LER model, the Godse and Gurland model is incapable of predicting the fracture toughness scatter.

The short reviews presented here show that there are two rivalling assumptions regarding cleavage fracture initiation. The more popular assumption is based on pure weakest link behaviour and leads to equation (12) for the fracture toughness scatter. The other assumption demands a certain critical fraction of the crack front to fracture to cause macroscopic crack propagation. In this case the models are incapable of predicting the fracture toughness scatter, because they contain no information regarding how the critical fraction differs from material to material, and specimen to specimen.

Fortunately the theory based on pure weakest link behaviour has been comparatively well verified by experimental data. For example, Wallin (29) and later Anderson and Stienstra (27) and Miyata, Otsuka, and Katayama (30) have shown with Monte Carlo simulation that the experimentally determined Weibull shape parameters in reality correspond to a value of four for K_{IC} (Fig. 2). The exact values for the confidence intervals obtained by the different

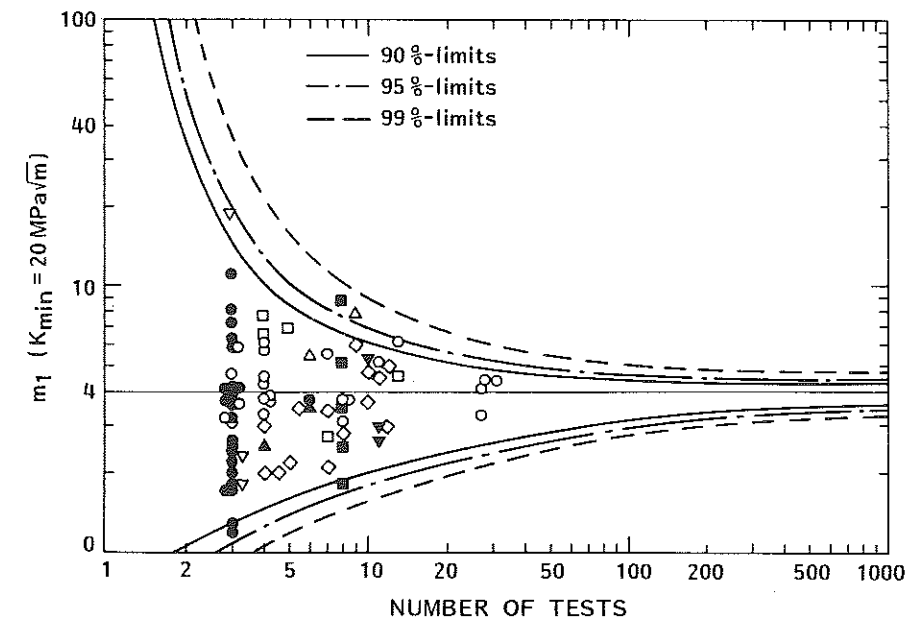


Fig 2 Theoretical scatter of experimentally determined values for the Weibull shape parameter as a function of the number of tests, when $K_{min} = 20 \text{ MPa}\sqrt{\text{m}}$ (29)

researchers are not exactly identical to each other, as the result is dependent upon the fitting procedure applied. Instead of using Monte Carlo simulation, the confidence intervals could be obtained from especially published tables. More on the subject can be found, for example, in (33). Additional experimental verification of the model based on single data sets have been obtained by several authors. Recently Urabe performed 30 CTOD tests on a low alloy steel (31). His results are presented in the form of K_δ values in Fig. 3. The K_δ values were estimated from Urabe's crack tip opening displacement values δ with $K_\delta^2 = E' \cdot m \cdot \sigma_y \cdot \delta$, where $m = 1.7$. The used K_{\min} of 23 MPa \sqrt{m} corresponds to his maximum pre-cracking stress intensity factor. Another large data set for A533B Cl. 1 steel has been presented by Neville (32). His data are plotted in a failure probability diagram in Fig. 4. Unfortunately Neville provides no information regarding the specimen size and pre-fatigue level. Miyata, Otsuka, and Katayama (30) performed 60 CTOD tests on SM 41 B steel. Their results are presented in the form of δ values in Fig. 5. Because $\delta \sim K^2$, i.e. $\delta_0 \gg \delta_{\min}$, δ_{\min} has been taken as zero for simplicity. The fact that part of the data in Fig. 5 corresponds to large-scale yielding does not seem to affect the scatter noticeably. Figures 3–5 also include the 90 percent confidence limits of the rank probabilities (33). In the case of K_1 (or \sqrt{J} or $\sqrt{\delta}$) the confidence limits are practically symmetrical (Figs 3 and 4), whereas in the case of J or δ (Fig. 5) the confidence of the rank estimates is not symmetrical.

The statistical thickness effect has also been quite well verified by Wallin (34) as well as others (e.g., (14)(23)(27)). Some of the most dramatic proofs of the thickness effect are depicted by a re-analysis of the ORNL thermal shock experiments (35), where the statistical thickness effect was used to describe the fracture toughness of the 1000 mm wide thermal shock cracks based on 25 mm

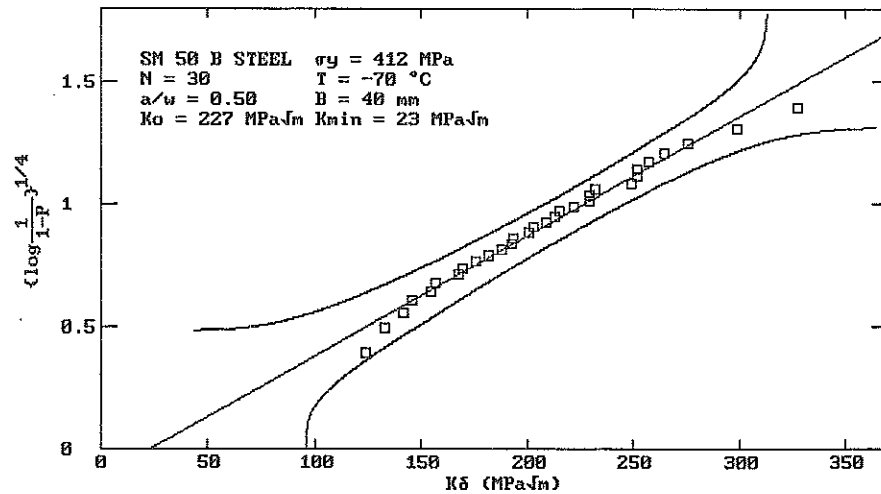


Fig 3 Urabe data (31) in the form of a failure probability diagram, with confidence limits for rank estimate

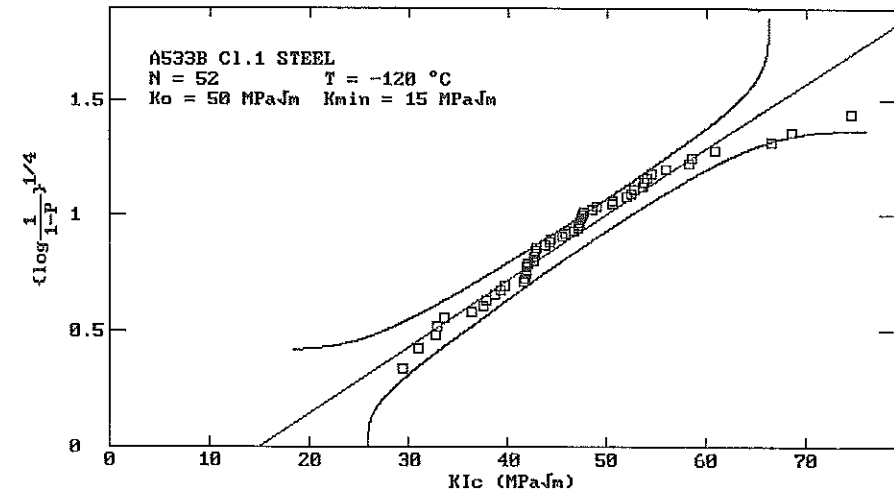


Fig 4 Neville data (32) in the form of a failure probability diagram, with confidence limits for rank estimate

CT specimen data (Figs 6–8). Figure 8 contain also size corrected data from 50 mm (2T) and 10 mm (CV) CT specimens. K_I corresponds to the elastic-plastic equivalent K_{Ic} calculated from the J -integral. In all cases it is seen that the size corrected CT specimen data describe the measured toughness of the 1000 mm wide cracks very well, with an exception for the upper transition region where the small specimen data is affected by large-scale yielding.

As shown above, the transition region is problematic. There, both large-scale yielding as well as ductile tearing may affect cleavage fracture. These combined

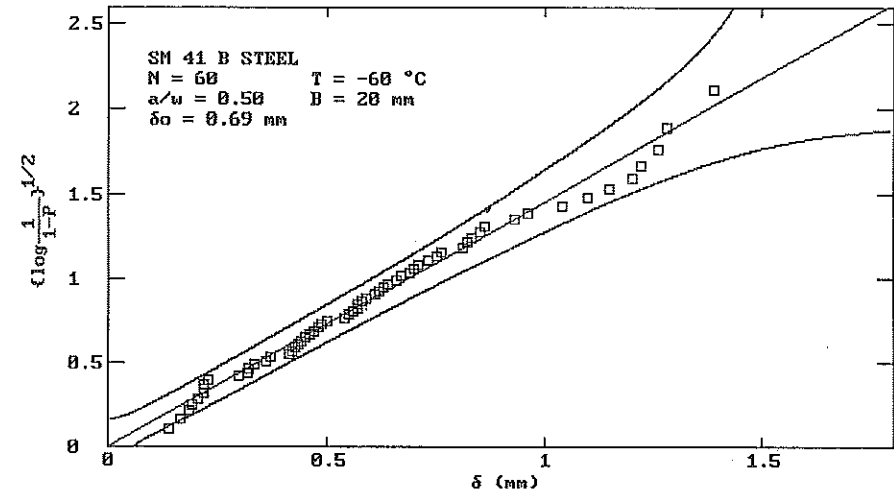


Fig. 5 Miyata *et al.* data (30) in the form of a CTOD based failure probability diagram, with confidence limits for rank estimate

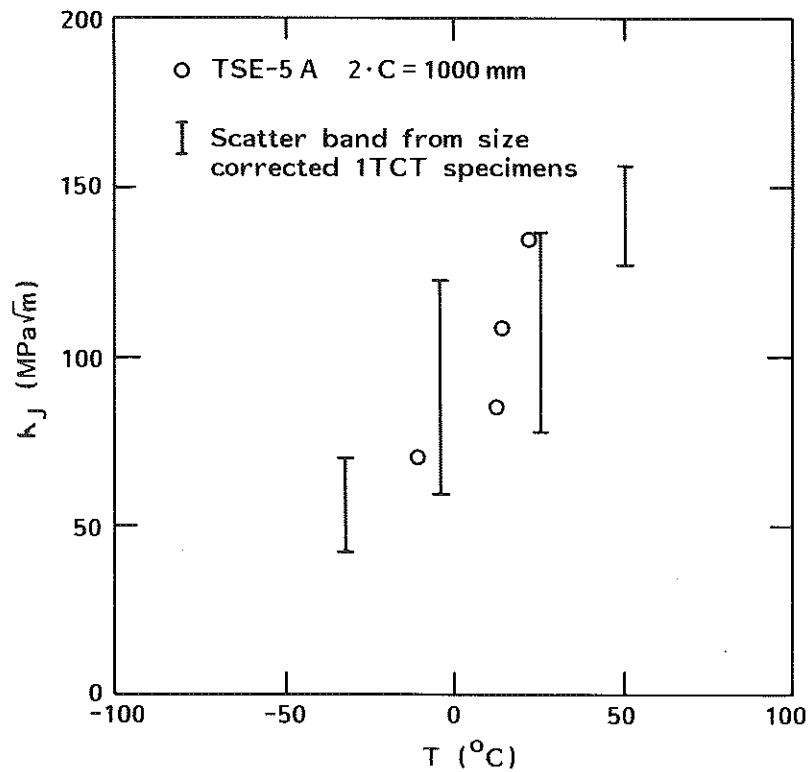


Fig 6 Statistical model based analysis of thermal shock experiment 5A material (35)

effects usually cause an apparent change in the shape parameter. Because the effects of the two factors are opposite in nature, they may in some cases yield a zero combined effect. This is probably the case with the Miyata, Otsuka, and Katayama data in Fig. 5. In order to model the fracture toughness scatter reliably also in the transition region both of these additional factors must be accounted for. Most existing models that have been developed for the transition region consider only one of them. Next, the effect of both factors will be examined separately.

Ductile crack growth correction (DCG)

The basic assumptions for the DCG correction (36) are presented schematically in Fig. 9. The distance parameter $\beta \sim x \cdot \sigma_{flow}^2 / K_I^2$ defines the cleavage fracture process zone size. In the derivation it is assumed that there exists a specific ductile fracture initiation toughness K_i and that the lower limiting fracture toughness K_{min} is zero. The sampling volume is presented as having a wedge shape with an active angle θ . The value of the angle and even the exact

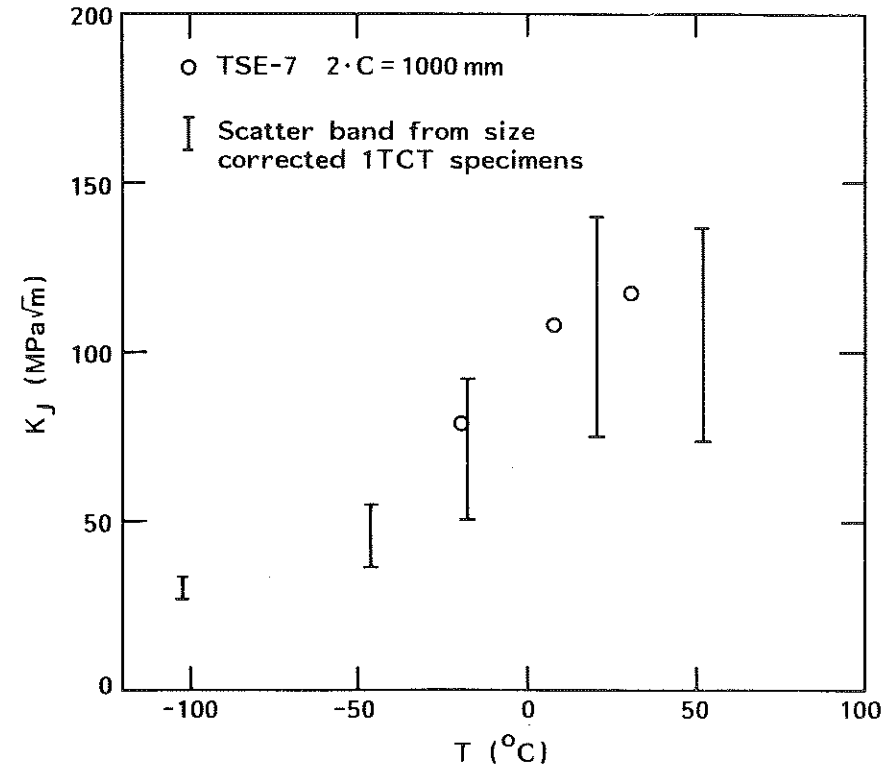


Fig 7 Statistical model based analysis of thermal shock experiment 7 material (35)

shape of the sampling volume is arbitrary. It is only used to show that the stress and strain distributions have an angular dependence. The stress distribution within the wedge in front of the crack is assumed to be insensitive to the crack growth. This assumption is based on the existing FEM analysis results.

Considering the fact that equation (12) actually describes a volume we can rewrite the equation as

$$P_f = 1 - \exp \left\{ - \left(\frac{V}{V_0} \right) \right\} \quad (18)$$

The volume increment due to both increase in loading parameter as well as crack growth is, when written as a function of Δa and neglecting second order terms

$$\partial V = \frac{V_i}{K_I^4} \cdot \{ 4 \cdot f(\Delta a)^3 \cdot f'(\Delta a) + 2 \cdot f(\Delta a)^2 \cdot \sigma_{flow}^2 / \beta \} \cdot \partial \Delta a \quad (19)$$

where $K_I = f(\Delta a)$.

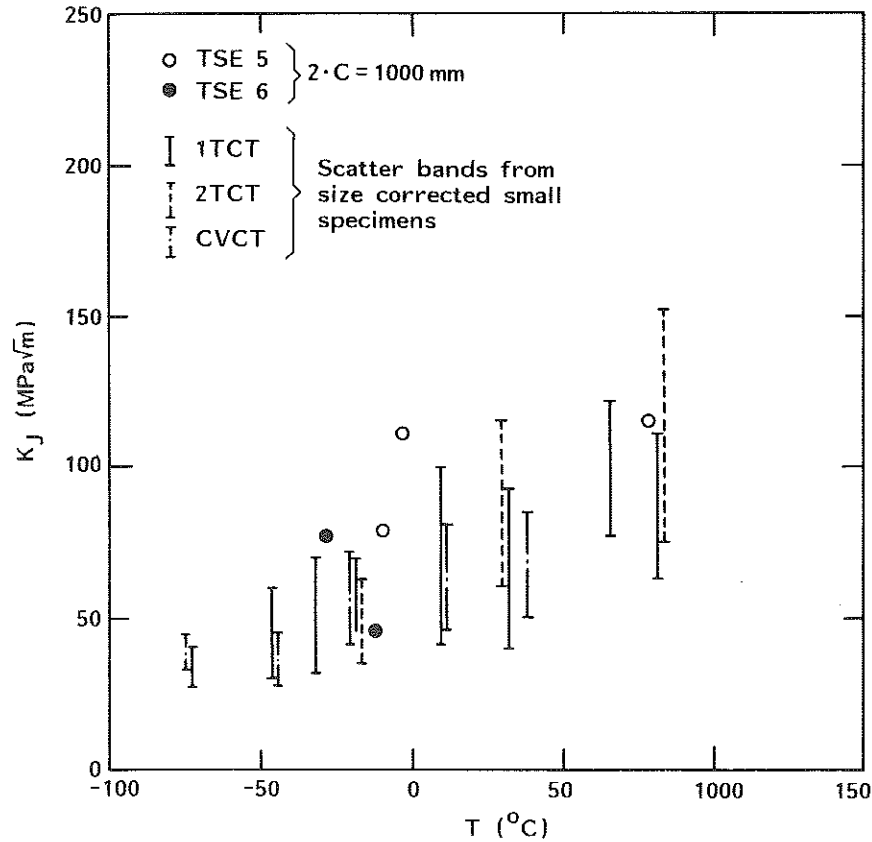


Fig 8 Statistical model based analysis of thermal shock experiments 5 and 6 material (35)

Integrating equation (19) and combining it with equation (18) the Δa correction becomes

$$\ln \frac{1}{1 - P_f} = \frac{f(\Delta a)^4}{K_0^4} + \frac{2 \cdot \sigma_{flow}^2}{K_0^4 \cdot \beta} \cdot \int_0^{\Delta a} f(\Delta a)^2 \cdot \partial \Delta a \quad (20)$$

for $K_I > K_I$.

The ductile crack growth correction presented here is not unique. Another DCG correction has been presented by Brückner and Munz (37). They have previously derived an expression for the ductile crack growth correction based on normal weakest link type Weibull statistics. When fixing the Weibull slope to be equal to 4, their expression becomes

$$\ln \frac{1}{1 - P_f} = \frac{K_I^4}{K_0^4} + \frac{1}{K_0^4 \cdot W_1} \cdot \int_0^{\Delta a} f(\Delta a)^4 \cdot \partial \Delta a \quad (21)$$

where W_1 is a constant, describing the size of the active volume in mm.

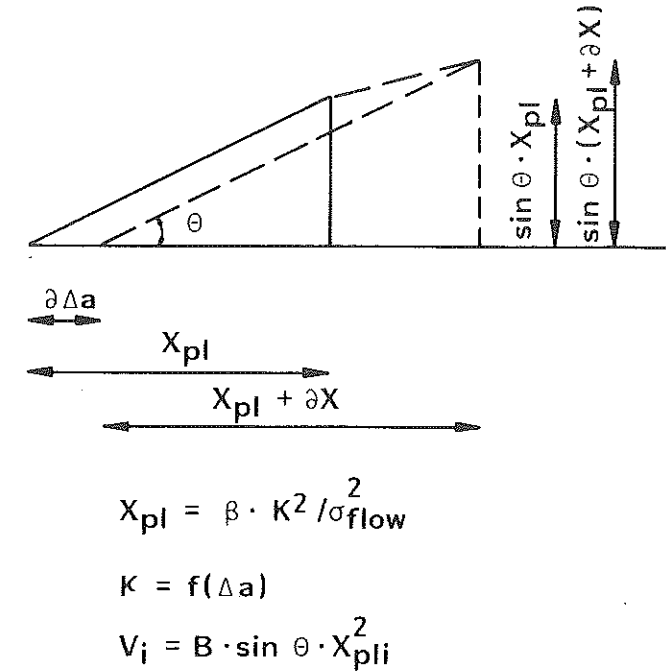


Fig 9 Schematic presentation of basic assumptions regarding ductile crack growth correction (36)

Ehl, Munz, and Brückner (38) have applied equation (21) on a very large set of data in the transition region. Unfortunately their model does not include the large-scale yielding effect.

Comparing equation (21) with equation (20) it is seen that they are rather similar. The difference in them is that the expression based on the general model assumes that the effective active volume continues to grow as a function of $(K_I^2)^2$ even after the ductile crack growth begins, whereas Brückner and Munz assume that the size of the active volume becomes constant when ductile crack growth starts.

The fitting capability of the two crack growth corrections is practically identical (36), but here, the assumption of the active volume being a function of $(K_I^2)^2$ is assumed because it seems logical to assume the plasticity to grow with increasing loading.

Both equations (20) and (21) have a drawback. They require that the crack growth integrals are solved. This means that the actual R curve up to cleavage fracture for each specimen must be known. Because there usually exists scatter in the ductile tearing R curves the application of equations (20) and (21) is either very laborious or demands the use of some mean approximation of the R curves. To overcome this difficulty a simplified form of the crack growth correction is required.

If the ductile crack growth is independent of K_I the crack growth correction is much simplified. It can be written as

$$\left(\ln \frac{1}{1-P_f}\right)^{1/4} = \frac{K_I}{K_0} \cdot \left(1 + \frac{2 \cdot \Delta a \cdot \sigma_{flow}^2}{K_I^2 \cdot \beta}\right)^{1/4} \quad (22)$$

When the crack growth is small ≈ 1 mm and/or the R curve is relatively flat, equation (22) can be used to approximate equation (20), by insertion of K_I in place of K_1 . When accounting for specimen thickness and a lower limiting fracture toughness the approximate correction becomes

$$\left(\ln \frac{1}{1-P_f}\right)^{1/4} = \frac{K_I - K_{min}}{K_0 - K_{min}} \cdot \left(\frac{B}{B_0}\right)^{1/4} \cdot \left(1 + \frac{2 \cdot \Delta a \cdot \sigma_{flow}^2}{K_I^2 \cdot \beta}\right)^{1/4} \quad (23)$$

Large-scale yielding of ligament (39)

Brittle cleavage fracture is a critical stress controlled local fracture process. The possible cleavage fracture initiators are randomly distributed and this causes cleavage fracture to be a statistical event. A pre-requisite for cleavage fracture is local plasticity at the site of fracture initiation. Therefore the process zone for cleavage fracture must be smaller than or equal to the plastic zone size. Because cleavage fracture is stress controlled, the probability of cleavage fracture initiation is largest close to the stress maximum. A somewhat refined version of the WST model (21) indicates that with a 95 percent probability, cleavage fracture will initiate closer to the crack tip than approximately 3–5 times the distance to the stress maximum. This can be taken as an effective process zone for cleavage fracture initiation. Outside this region cleavage fracture is still in theory possible within the plastic zone, but the probability of fracture as compared to the fracture probability closer to the stress maximum is essentially negligible.

The J -integral or K_J describes cleavage fracture initiation as long as it describes the stresses within the process zone with an adequate accuracy. McMeeking and Parks (40) showed with their FEM calculations that at increasing J levels the stresses start to deviate from the small-scale yielding calculations. They plotted their results in the form of the normalised distance $x/(J/\sigma_0)$ to be able to make the comparison with the small-scale yielding results. With increasing J the stresses deviated from the small-scale yielding results at smaller values of normalised distance. When the process zone is defined with the normalised distance it is possible to determine the ligament size and J level at which the stresses no longer describe the process zone correctly. If the cleavage fracture initiation process zone extends to approximately 3–5 times the distance of the stress maximum the McMeeking and Parks results would indicate that the size restriction $b \geq \alpha \cdot (J/\sigma_0)$ should be $b \geq 35-60 \cdot (J/\sigma_0)$. It should be pointed out that the size restriction for cleavage is not the same as the standard size restriction for ductile fracture ($\alpha \approx 25$).

Besides having a ligament size restriction it is equally interesting to know what happens to the stresses at higher load levels. In order to investigate this the McMeeking and Parks results were replotted in coordinates where the distance is normalised with the ligament and not by J . The thus obtained results are presented in Fig. 10. It is seen that the stress distribution above a certain load level saturates and becomes independent of J , and depends only

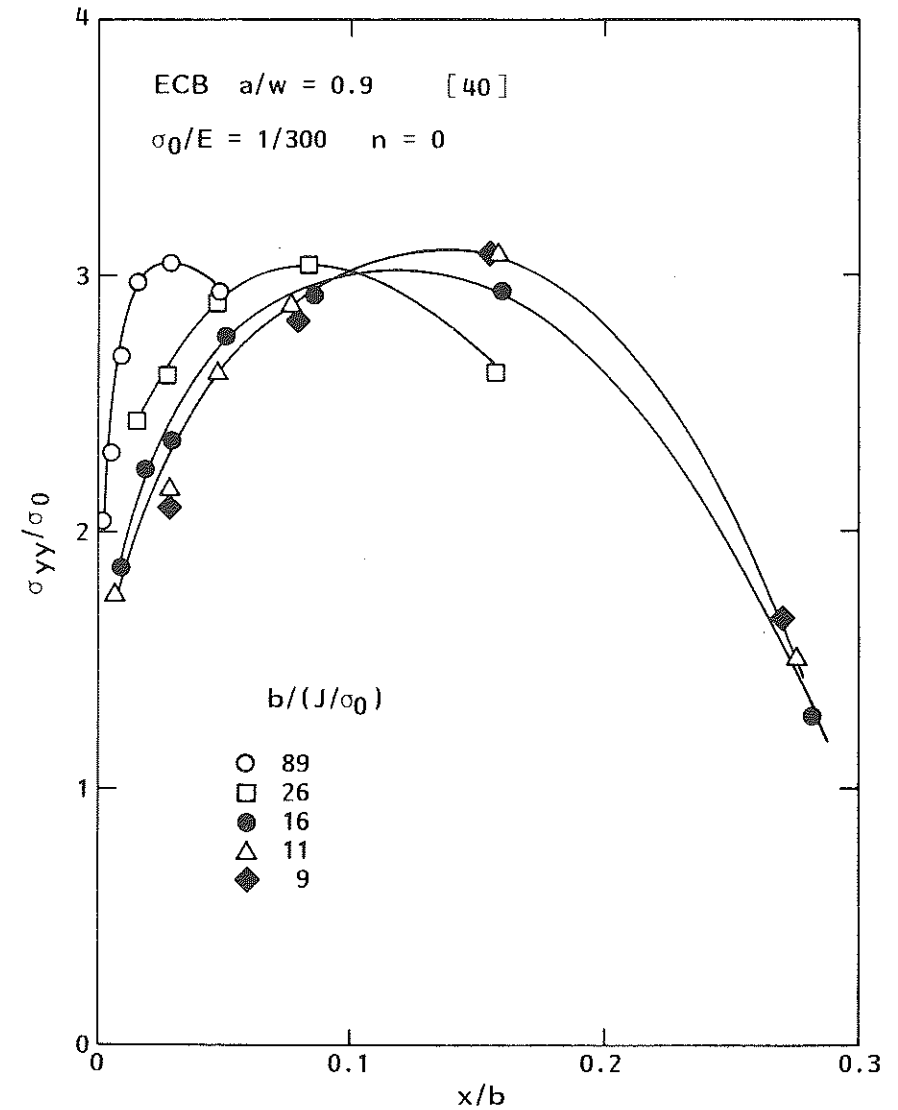


Fig 10 Stress distribution in front of crack for large-scale yielding (40)

on ligament size. This means that beyond a certain critical J -value the effective J from a cleavage fracture point of view becomes constant.

The effect of large-scale yielding can also be investigated by re-analysing the FEM calculations by Mudry and co-workers (14)(41). They apply the Beremin model (12) based on Weibull statistics combined with large-scale yielding FEM calculations of a CT specimen. The results are interpreted in the form of an effective Weibull stress which for small-scale yielding is defined as $\sigma_w \sim (K_I^4 \cdot B)^{1/m}$, where B is the specimen thickness and m is the Weibull shape parameter. They determine a J validity criteria as the load level where the large-scale yielding σ_w deviates more than 7 percent from the theoretical small-scale yielding result. Another possibility of how to analyse their results is to make use of the theoretical small-scale yielding definition of σ_w and to turn the large-scale yielding results directly into an effective K_I value. One re-analysed result for a CT specimen is presented in Fig. 11. Here the same behaviour as in Fig. 10 is visible. First, at low K_j levels, the effective $K_{j,eff}$ is equal to the measured K_j , but above a certain level $K_{j,eff}$ saturates and finally becomes constant. The saturation level corresponds to a maximum J_{max} that yields a size criterion of approximately $b = 50 \cdot (J_{max}/\sigma_{flow})$. This is well in accordance with the assumption of a cleavage fracture initiation process zone having a size of 3–5 times the distance to the stress maximum which led to a size criterion of $b \geq 35-60 \cdot (J/\sigma_0)$.

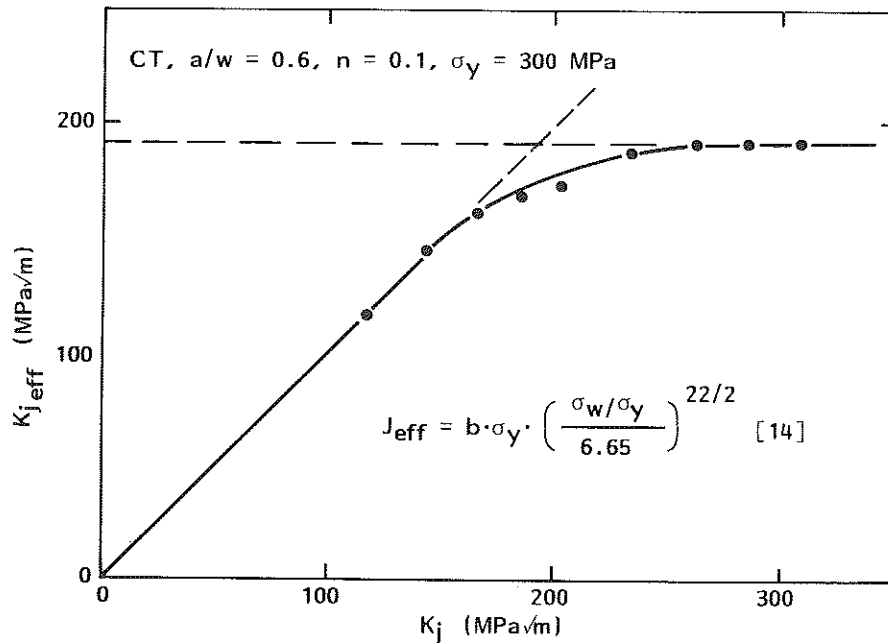


Fig 11 Relation between K_j and $K_{j,eff}$ (14)

With the foregoing discussions in mind, the following assumptions regarding the effect of ligament size on cleavage fracture toughness are proposed:

- the J integral (or K_j) describes the cleavage fracture initiation event as long as $b \geq 50 \cdot (J/\sigma_{flow})$;
- at higher load levels the effective load parameter J_{eff} is constant and equal to $J_{max} = b \cdot \sigma_{flow}/50$;
- when J_{eff} reaches J_{max} ductile tearing will precede cleavage fracture initiation.

As already mentioned, Mudry and co-workers also determined a ligament size limitation for cleavage fracture initiation (14)(41). They did not do the calculations in the form of K_I or J , but in the form of the so-called Weibull stress defined in the Beremin model (12). Thus their results are not so easy to analyse. The Beremin model has also been used by Amar and Pineau (42) to describe the large-scale yielding effect in the transition region. Their stress analysis is based directly on FEM analysis, but they do not consider the statistical effect of crack propagation. Unfortunately their results are not suitable for a re-analysis on the basis of the derivations presented here. This is due to the fact that they used cracked round tensile specimens. For this specimen type the crack circumference is not constant, but changes as a function of crack growth. Even in the simple case of small-scale yielding and no crack growth equation (13) is not valid for these types of specimens. This is because equation (13) assumes a constant thickness in front of the crack. For the round tensile specimens the effective thickness is analogous to $B = 2 \cdot \pi \cdot (R_0 - x)$, where x is the distance in front of the crack. When this is inserted into equation (9) the result will be considerably more complicated than equations (12) or (13). The resulting equation can be expressed roughly as

$$P_f = 1 - \exp - \{ \text{const}_1 \cdot R_0 \cdot K_I^4 - \text{const}_2 \cdot K_I^6 \} \quad (24)$$

Only if $R_0 \gg (K_I/\sigma_y)^2$, will equation (24) reduce to equation (12).

Satoh, Toyoda, and Minami (STM) have tried to develop a model for large-scale yielding (43). They define $P(a \geq a_c)$ with the two parameter Weibull distribution function and assume that the cleavage fracture process zone size is constant in large-scale yielding. However, they assume that the stresses are still described by the HRR field. These assumptions contain a discrepancy. The cleavage fracture process zone is determined by the stress distribution and therefore the process zone size should not be constant if the stresses are described by the HRR field. Furthermore, STM do not consider the statistical effect of crack propagation. Thus the STM approach does not seem directly suitable for describing the transition region.

Anderson (44), equivalently to the present analysis, defines an effective J_{yy}^* value based on the actual stress distribution, but his analysis does not include crack growth.

Next an attempt is made to verify the theoretical assumptions presented here also experimentally.

Experimental verification

The experimental verification consisted of 105 K_{Jc} tests with identical specimens (39). All specimens were tested at room temperature and the value of the J -integral at cleavage fracture initiation as well as the amount of ductile tearing were recorded. The results are presented as a multispecimen J - R curve in Fig. 12.

Equation (22) implies that if $K_{j_{eff}}$ is constant, one will obtain a linear function of ductile crack growth. The results are shown in Fig. 13. After a ductile crack growth of approximately 0.6 mm the fracture behaviour is exactly as predicted through equation (22). This confirms the assumption of a constant effective load parameter. The next step is to try to determine the value of $K_{j_{max}}$.

If one considers only specimens without ductile tearing $K_{j_{eff}}$ should be equal to K_j and equation (13) can be applied. The present results showing no ductile tearing are presented in Fig. 14. The experimental results describe equation (13) rather well when considering the confidence of the rank analysis.

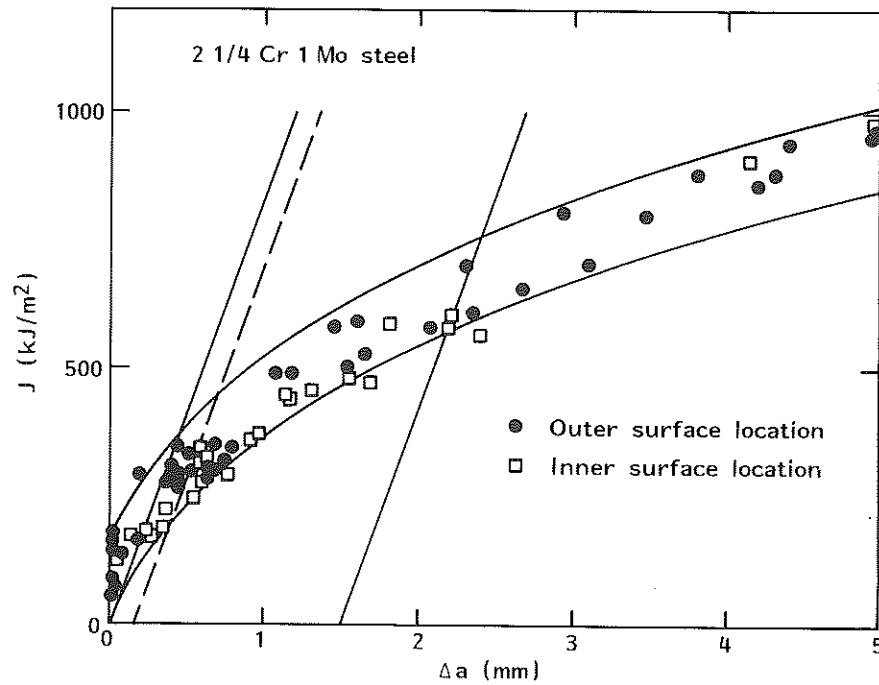


Fig 12 Fracture toughness results. Points and squares correspond to cleavage fracture initiation (39)

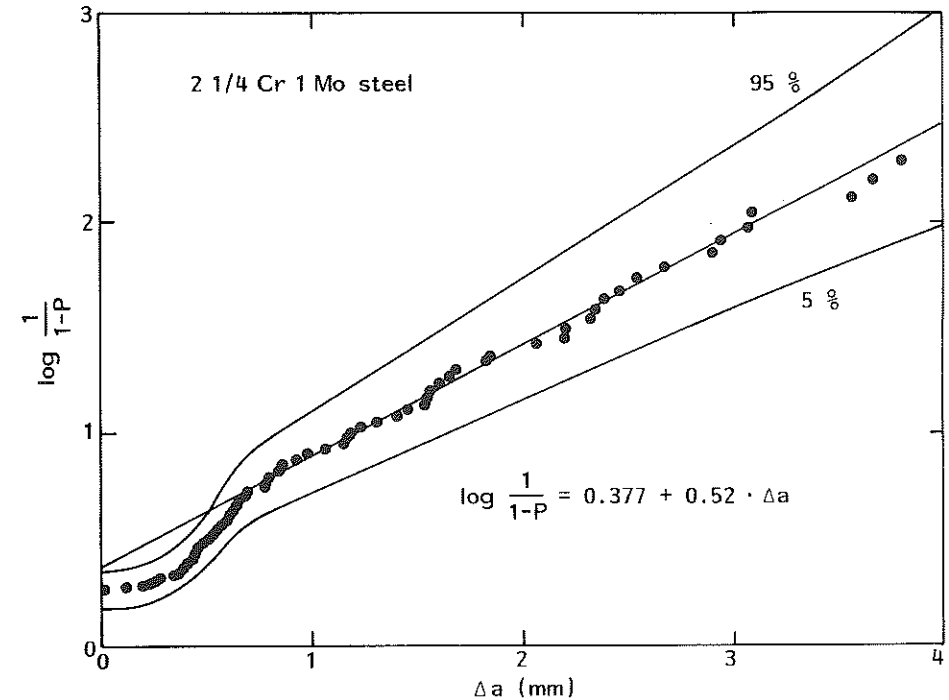


Fig 13 Fracture probability versus ductile crack growth with confidence limits for rank estimate (39)

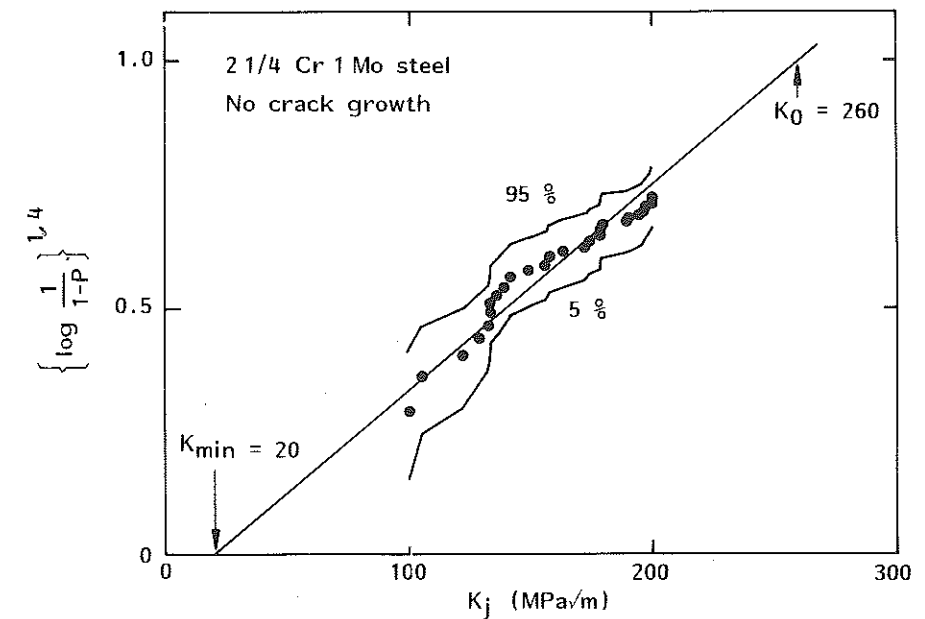


Fig 14 Fracture probability versus fracture toughness with confidence limits for rank estimate (39)

The presentation of the confidence limits in Fig. 14 differs from the presentation in the other figures. Here, instead of drawing the confidence limits as smooth lines with reference to the fitted median line as described in (33), the confidence limits are expressed with reference to the median rank estimate for each individual test result, thus producing irregular lines. For the first type of presentation the experimental results should lie within the confidence lines, whereas for the second type of presentation the median fitted line should lie within the confidence limits. Both types of presentation are equally well applicable. The results yield that $K_{\min} \approx 20 \text{ MPa}\sqrt{\text{m}}$ and $K_0 \approx 260 \text{ MPa}\sqrt{\text{m}}$. When this information is combined with the information in Fig. 13 one obtains that $K_{j\max} \approx 208 \text{ MPa}\sqrt{\text{m}}$, which corresponds to $\alpha \approx 44$ and $\beta \approx 0.0058 = 5.3 \cdot U_{\max}$, with U_{\max} equal to the normalised distance to the stress maximum from the crack tip.

The analysis can also be performed directly on the combined data, by using equation (23) and by applying $K_{j\text{eff}}$ instead of K_j . $K_{j\text{eff}}$ is then either equal to K_j or $K_{j\max}$ depending on the value of K_j . A best fit of all the data yields $K_{\min} \approx 20 \text{ MPa}\sqrt{\text{m}}$, $K_0 \approx 244 \text{ MPa}\sqrt{\text{m}}$, $K_{j\max} \approx 169 \text{ MPa}\sqrt{\text{m}}$ ($\alpha \approx 65$) and $\beta \approx 0.0037 = 3.4 \cdot U_{\max}$.

It is seen that the experimental estimates of both the size requirement (α), as well as the cleavage fracture initiation process zone size (β), are comparatively close to the theoretical assumptions. Therefore it is possible to fix α as 50, β as $3.5 \cdot U_{\max}$, and K_{\min} as $20 \text{ MPa}\sqrt{\text{m}}$. Thus the only parameter to fit is the normalisation toughness K_0 .

The results of the analysis of the present material are presented in Fig. 15. In this figure the 5 and 95 percent confidence limits of the rank based probabilities are included. The data are seen to be well described through the simplified crack growth correction. The standard deviation of the estimates of rank probabilities is 0.03.

The model is applied on three other materials. In Figs 16 and 17 data by Iwodate (45) have been analysed by equation (21) by using $\alpha = 50$ and $\beta = 3.5 \cdot U_{\max}$ (36). The third material relates to Ehl, Munz, and Brückner (38) and Brückner-Foit, Ehl, Munz, and Trolldenier (46). They found that for all geometries tested there were no fracture initiation sites within a distance of about 1 mm from the specimen surface. Thus one should really use the thickness reduced by 2 mm for the thickness correction. Usually this is not necessary, but for very thin specimens with $B < 10 \text{ mm}$ the effect must be accounted for. In Fig. 18 the data, corrected for specimen thickness, have been presented as a function of crack growth.

The thickness correction yields a very good normalisation of the data. Furthermore it is seen that in the large-scale yielding situation the data again yield a linear function of ductile crack growth.

Based on Monte Carlo simulation the theoretical expectance value together with the 90 percent confidence limits for the standard deviation of the estimates of rank probabilities were determined as a function of number of tests N .

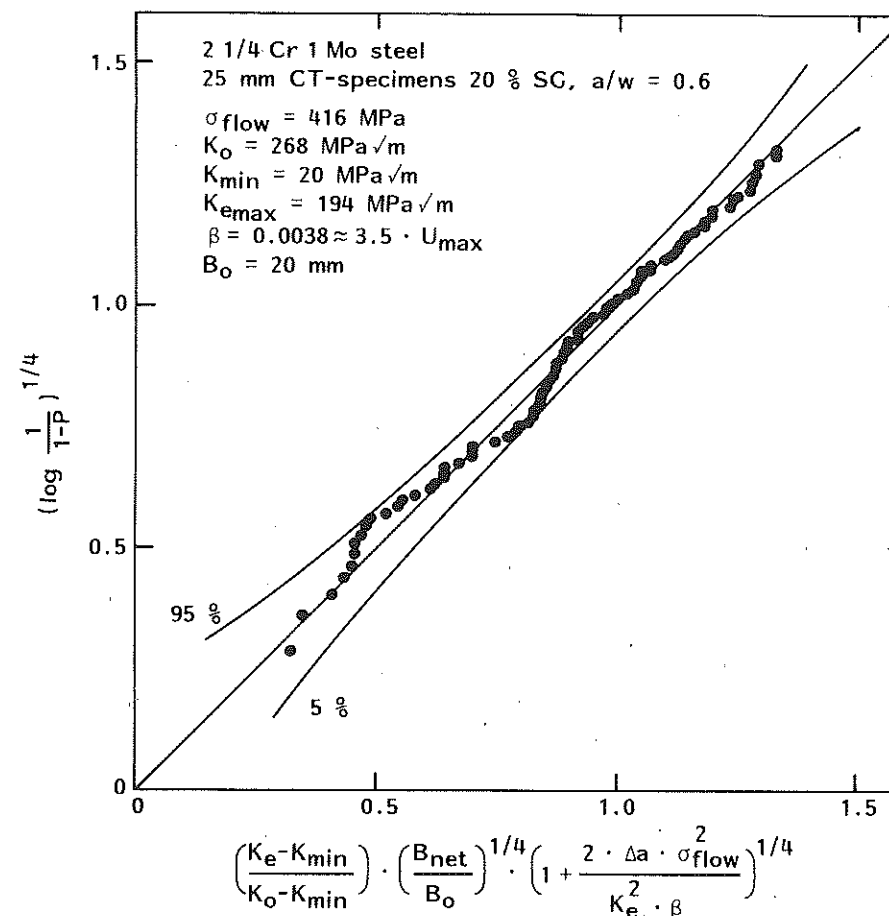


Fig 15 Crack growth correction analysis for 105 specimens (36)

The result describes the theoretical accuracy of a fit that is based on rank probabilities. The results of the simulation are presented in Fig. 19 together with the result of the present analysis as well as results for several other data sets found in the literature (47).

Considering the fact that equation (23) is merely a crude approximation and theoretically applicable only for macroscopically homogeneous materials, the present results are more than satisfactory. On the whole the results are quite promising and they would indicate that the statistical crack growth correction presented here is realistic. It also seems that 'macroscopical' inhomogeneities in the base material do not have a pronounced effect on the fracture toughness distribution.

The exact values for α and β cannot be reliably determined here and it is not

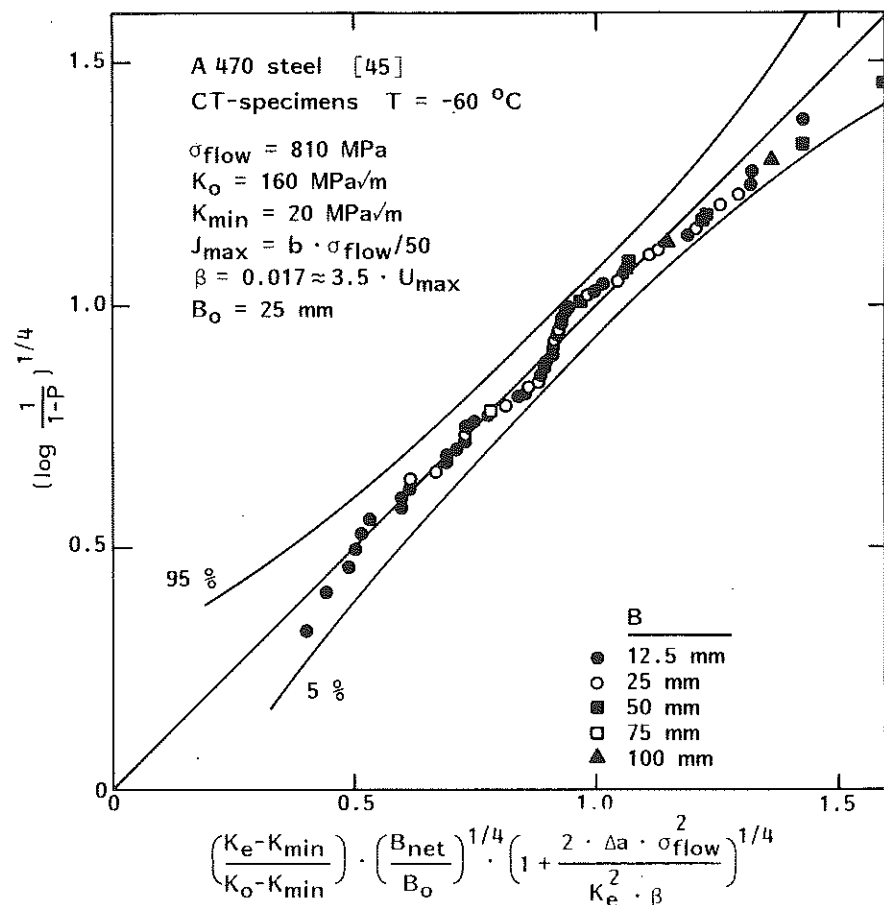


Fig 16 Crack growth correction analysis for 63 specimens (36)(45)

known how they will change from one material to another, but it is felt that one can with sufficient accuracy apply $\alpha = 50$ and $\beta = 3.5 \cdot U_{\text{max}}$.

The fact that equation (23) yields a correct description of the brittle fracture probability has widespread effects regarding fracture toughness testing in the ductile/brittle transition temperature region. It means that it is possible to use quite small specimens for the tests, the results of which can then be transformed to represent the behaviour of a large specimen or a structural detail. The correction for a single test can be expressed as

$$K_{\text{large}} = K_{\text{min}} + (K_{\text{jeff}} - K_{\text{min}}) \cdot \left(\frac{B}{B_{\text{large}}}\right)^{1/4} \cdot \left(1 + \frac{2 \cdot \Delta a \cdot \sigma_{\text{flow}}^2}{K_{\text{jeff}}^2 \cdot \beta}\right)^{1/4} \quad (25)$$

where K_{large} and B_{large} correspond to the corrected result.

As an example of its applicability, the ORNL pressurised thermal shock

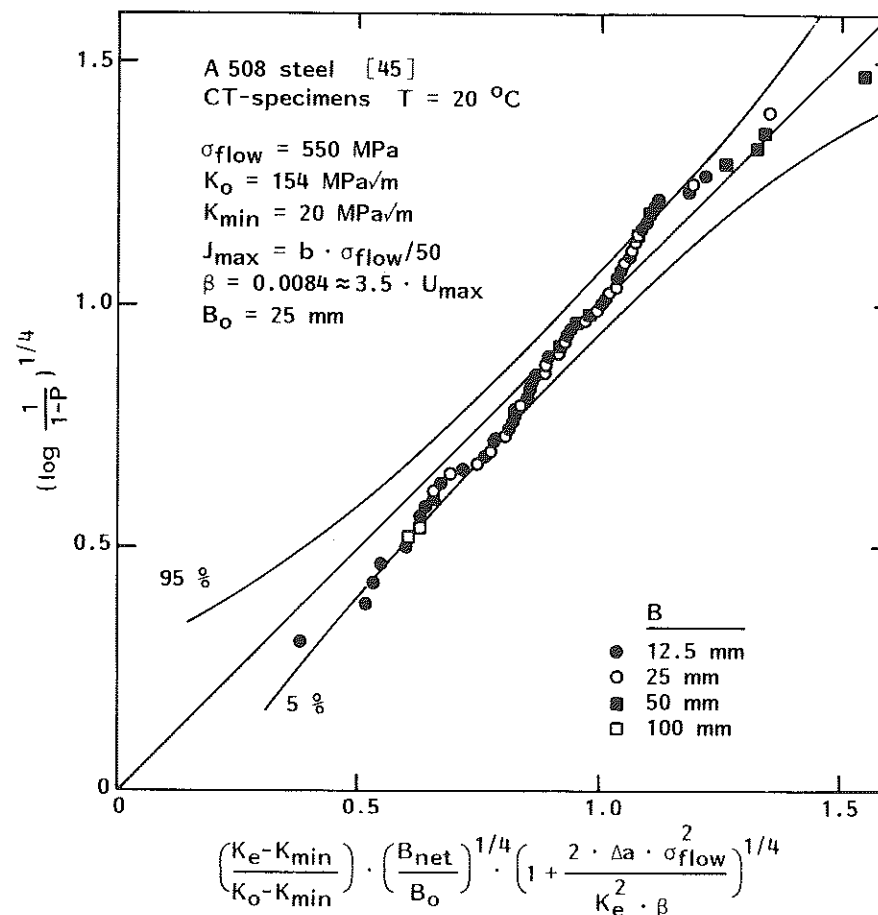


Fig 17 Crack growth correction analysis for 78 specimens (36)(45)

experiment, two results have been analysed by equation (25) in Fig. 20 (35). Here, the small specimen (25 mm CT) data were corrected to correspond to the actual 1000 mm wide crack, including the effect of large-scale yielding and ductile tearing. For comparison also the deterministic ORNL analysis where the small specimen data have been treated with the empirical Irwin/Merkle β -correction is presented in Fig. 21 (48). The constraint based β correction, assumed to give a lower bound toughness, yields in this case actually an unconservative estimate of the fracture behaviour of a 1000 mm wide crack.

Summary and conclusions

It can be concluded that the weakest link based statistical approach to cleavage fracture initiation offers effective means of analysing fracture toughness

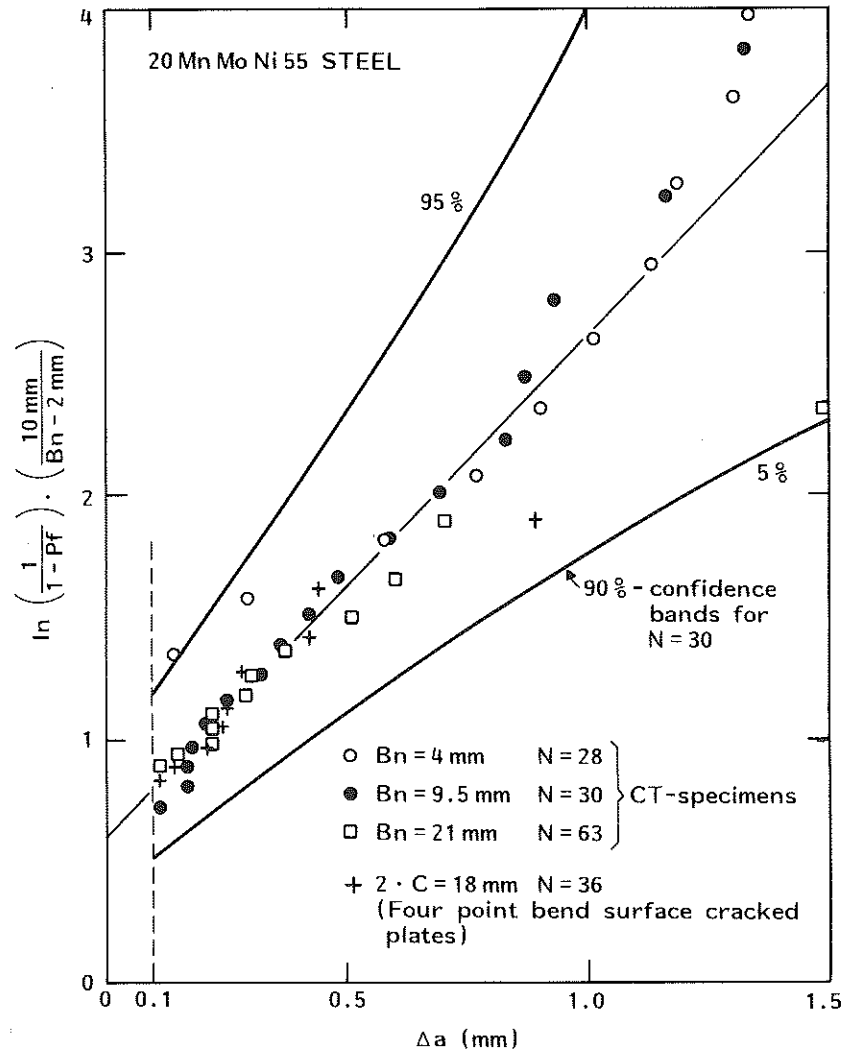


Fig 18 Thickness corrected failure probability diagram in the form of crack growth. Data from (38)(46)

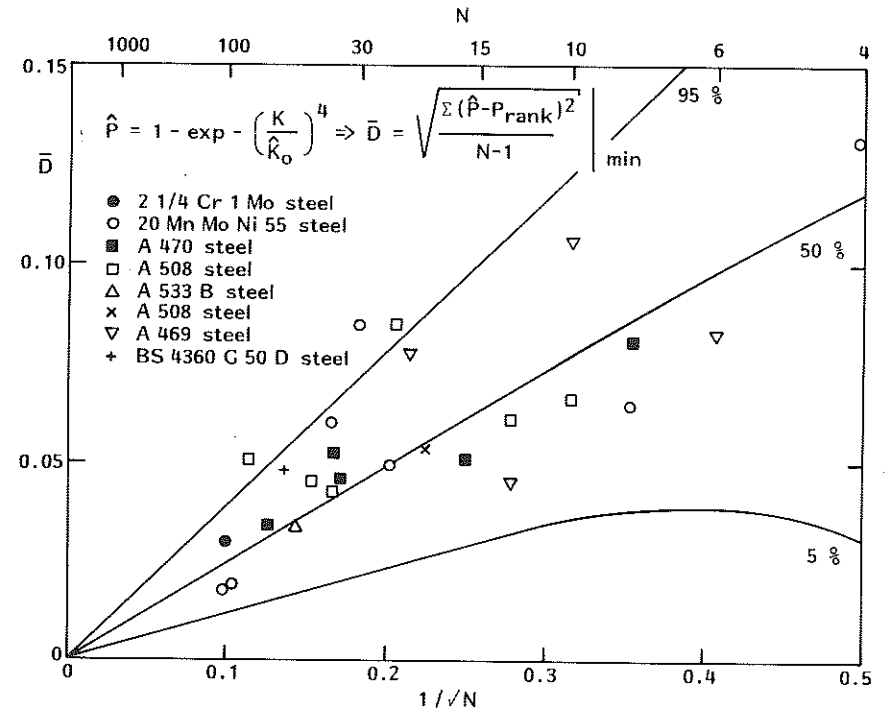


Fig 19 Theoretical 90 percent confidence limits for the standard deviation of the estimates of rank probabilities as a function of number of tests N (47)

data. The model assuming pure weakest link behaviour has been adequately verified for the lower shelf region. Here the model can be used to develop statistically sound safety factors to be used in failure assessment codes.

For use in the ductile-to-brittle transition region a simple large-scale yielding correction has been presented. When combined with a ductile crack growth correction it can be used to describe the scatter and thickness effect of fracture toughness. The model has a strong impact on standard development for fracture toughness testing in the ductile-brittle transition region.

Despite the excellent results that have been obtained by the model, much work is still needed to make precise the values of the cleavage fracture process zone size and the ligament size requirement.

Acknowledgements

This work is a part of the Structural Materials in Nuclear Power Plant programme performed at the Technical Research Centre of Finland (VTT) and financed by the Ministry of Trade and Industry in Finland. Additional financing by the Academy of Finland is acknowledged.

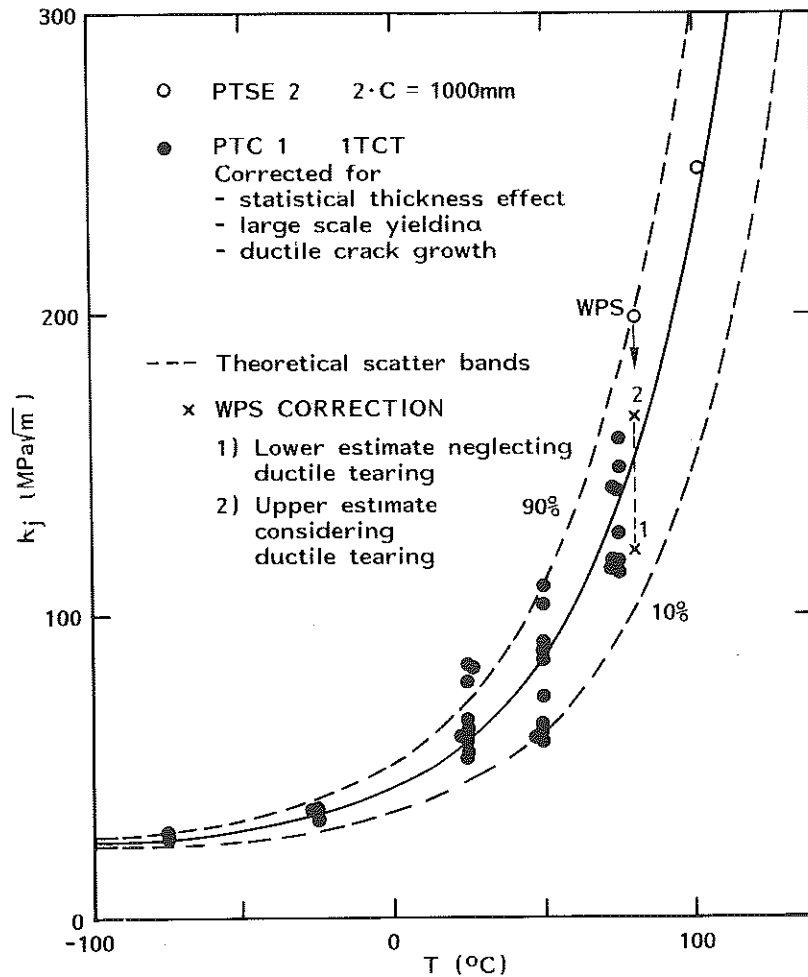


Fig 20 Equation (23) based analysis of ORNL pressurised thermal shock experiment 2 material (35)

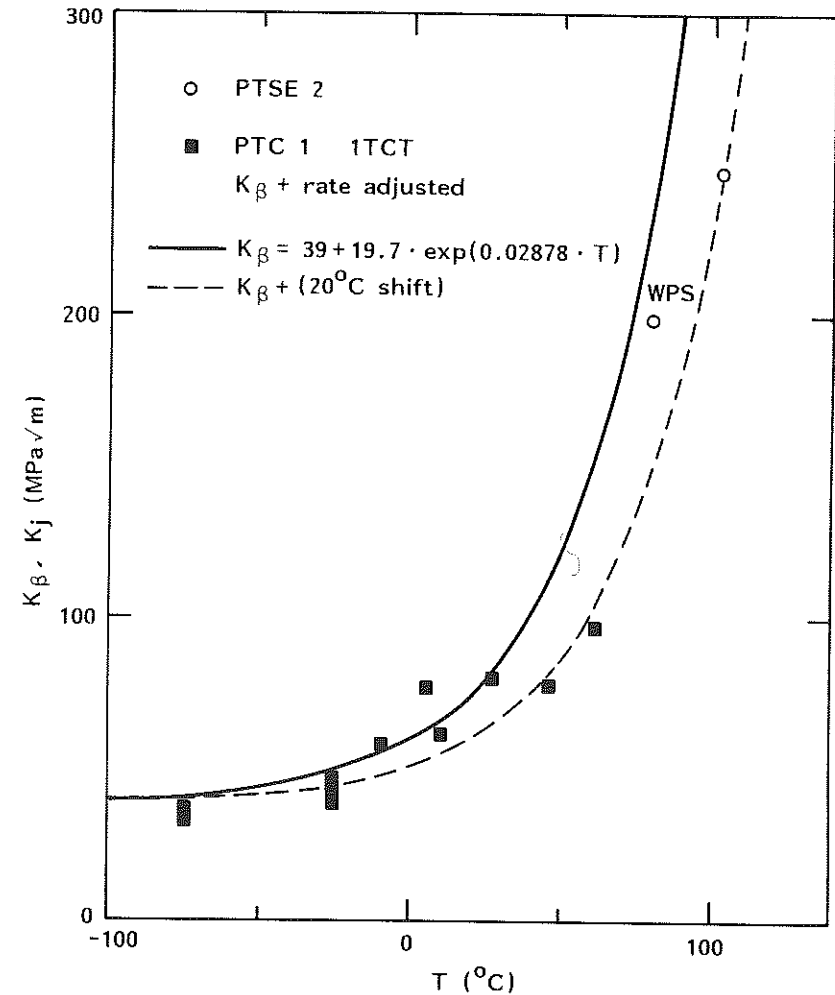


Fig 21 Original analysis of the PTSE 2 material based on rate adjusted β -correction (48)

References

- (1) WALLIN, K. (1987) A quantitative statistical model for cleavage fracture initiation in carbide strengthened steels, PhD thesis, Espoo.
- (2) RITCHIE, R. O., KNOTT, J. F., and RICE, J. R. (1973) On the relationship between critical tensile stress and fracture toughness in mild steel. *J. Mech. Phys Solids*, **21**, 395-410.
- (3) CURRY, D. A. and KNOTT, J. F. (1979) Effect of microstructure on cleavage fracture toughness of quenched and tempered steels, *Met. Sci.*, **13**, 341-345.
- (4) BRÜCKNER-FOIT, A., MUNZ, D., and TROLLDENIER, B. (1989) Arbeitsbericht zum DFG Vorhaben 'Sprödbruch' MU466/14-1, Zeitraum vom 1.07.1987-31.12.1988 Institut für Zuverlässigkeit und Schadenkunde im Maschinenbau, Universität Karlsruhe (TH), Karlsruhe, 45.
- (5) TOIVONEN, J. (1987) The effect of mechanical loading on acoustic emission in a fracture toughness test, (in Finnish) M.Sc. Thesis, Helsinki Technical University, Espoo.

- (6) CURRY, D. A. (1980) Comparison between two models of cleavage fracture, *Met. Sci.*, **14**, 78–80.
- (7) LANDES, J. D. and SHAFFER, D. H. (1980) Statistical characterization of fracture in the transition region, *Fracture Mechanics: Twelfth Conference, ASTM STP 700*, pp. 368–382, ASTM, Philadelphia.
- (8) ANDREWS, W., KUMAR, V., and LITTLE, M. M. (1981) Small-specimen brittle-fracture toughness testing, *Fracture Mechanics: Thirteenth Conference, ASTM STP 743*, (Edited by R. Roberts), pp. 576–598, ASTM, Philadelphia.
- (9) BRÜCKNER, A. and MUNZ, D. (1983) Prediction of failure probabilities for cleavage fracture from the scatter of crack geometry and of fracture toughness using the weakest link model, *Engng. Fracture Mech.*, **18**, 359–375.
- (10) SATOH, K., TOYODA, M., and MINAMI, F. (1985) A probabilistic approach to evaluation of fracture toughness of welds with heterogeneity, *Trans Japan Welding Soc.*, **16**, 70–81.
- (11) LANDES, J. D. and McCABE, D. E. (1984) Effect of section size on transition temperature behavior of structural steels, *Fracture Mechanics: Fifteenth Symposium, ASTM STP 833*, (Edited by R. J. Sanford), pp. 378–392, ASTM, Philadelphia.
- (12) BEREMIN, F. M. (1983) A local criterion for cleavage fracture of a nuclear pressure vessel steel, *Met. Trans.*, **14A**, 2277–2287.
- (13) PINEAU, A. (1981) Review of fracture micromechanisms and a local approach to predicting crack resistance in low strength steels, *Advances in Fracture Research, 5th International Conference on Fracture*, (Edited by D. Francois), **2**, pp. 553–577.
- (14) MUDRY, F. (1986) A local approach to cleavage fracture, *Seminaire International sur L'Approche Locale de la Rupture*, Moret-sur-Loing, 165–186.
- (15) QU, D., WANG, X. W., and TSAI, C. K. (1983) On the weibull model of cleavage fracture, *Mech. Behavior of Materials – IV (ICM 4)*, (Edited by J. Carlsson and N. G. Ohlson), **2**, pp. 779–785.
- (16) HOU, C., CAI, Q., SU, Y., and ZHENG, X. (1984) Volume effect on cleavage strength, microstructure and fracture micromechanism of welded 15MnVN steel, *Advances in Fracture Research (Fracture 84), 6th International Conference on Fracture*, (Edited by S. R. Valluri, D. M. R. Taplin, P. Rama Rao, J. F. Knott, and R. Dubey), vol. 2, pp. 1415–1422.
- (17) EVANS, A. G. (1983) Statistical aspects of cleavage fracture in steel, *Met. Trans.*, **14A**, 1349–1355.
- (18) WALLIN, K., SAARIO, T., TÖRRÖNEN, K., and FORSTÉN, J. (1983) A microstatistical model for carbide induced cleavage fracture, Technical Research Centre of Finland, Research Reports 220, Espoo, 15.
- (19) TÖRRÖNEN, K., WALLIN, K., SAARIO, T., HÄNNINEN, H., RINTAMAA, R., and FORSTÉN, J. (1985) Optimization of metallurgical variables in fracture prevention, *Nucl. Engng Des.*, **87**, 225–237.
- (20) WALLIN, K., SAARIO, T., and TÖRRÖNEN, K. (1987) Fracture of brittle particles in a ductile matrix, *Int. J. Fracture*, **32**, 201–209.
- (21) SAARIO, T., WALLIN, K., and TÖRRÖNEN, K. (1984) On the microstructural basis of cleavage fracture initiation in ferritic and bainitic steels, *J. Engng Mater. Technol.*, **106**, 173–177.
- (22) VEISTINEN, M. K. and WALLIN, K. (1986) Cleavage fracture in 26Cr-1Mo ferritic stainless steel, *Mater. Sci. Technol.*, **2**, 666–670.
- (23) SLATCHER, S. (1986) A probabilistic model for lower-shelf fracture toughness – theory and application, *Fatigue Fracture Engng Mater. Structures*, **9**, 275–289.
- (24) LIN, T., EVANS, A. G., and RITCHIE, R. O. (1986) A statistical model of brittle fracture by transgranular cleavage, *J. Mech. Phys Solids*, **34**, 477–497.
- (25) TYSON, R. T. and MARANDET, B. (1988) Cleavage toughness variability and inclusion size distribution of a weld metal, *Fracture Mechanics: Eighteenth Symposium, ASTM STP 945*, (Edited by D. T. Read and R. P. Reed), pp. 19–32, ASTM, Philadelphia.
- (26) ANDERSON, T. L. (1989) A combined statistical and constraint model for the ductile-brittle transition region, *Nonlinear Fracture Mechanics: II – Elastic-Plastic Fracture, ASTM STP 995*, (Edited by J. D. Landes, A. Saxena, and J. G. Merkle), pp. 563–583, ASTM, Philadelphia.
- (27) ANDERSON, T. L. and STIENSTRA, D. (1989) A model to predict the sources and magnitude of scatter in toughness data in the transition region, *J. Testing Evaluation*, **17**, 46–53.
- (28) GODSE, R. and GURLAND, J. (1989) A statistical model for low temperature cleavage fracture in mild steels, *Acta Met.*, **37**, 541–548.
- (29) WALLIN, K. (1984) The scatter in K_{IC} -results, *Engng. Fracture Mech.*, **19**, 1085–1093.
- (30) MIYATA, T., OTSUKA, A., and KATAYAMA, T. (1988) Probabilistic analysis of cleavage fracture and fracture toughness of steels, (in Japanese) *J. Soc. Mat. Sci., Japan*, **37**, 1191–1196.
- (31) URABE, N. (1989) Statistical studies on fracture toughness of steels, *Statistical Research on Fatigue and Fracture: Current Japanese Materials Research*, **2**, (Edited by T. Tanaka, S. Nishijima, and M. Ichikawa), pp. 105–123.
- (32) NEVILLE, D. (1987) Statistical analysis of fracture toughness data, *Engng. Fracture Mech.*, **27**, 143–151.
- (33) WALLIN, K. (1989) Optimized estimation of the weibull distribution parameters, Technical Research Centre of Finland, Research Reports, **604**, Espoo.
- (34) WALLIN, K. (1985) The size effect in K_{IC} -results, *Engng. Fracture Mech.*, **22**, 149–163.
- (35) TÖRRÖNEN, K., AALTONEN, P., HÄNNINEN, H., KAUPPINEN, P., KEINÄNEN, H., RINTAMAA, R., WALLIN, K., and VALO, M. (1988) Overview of the recent results of the safety related research in pressure boundary components of Finnish nuclear power plants, Technical Research Centre of Finland (VTT), Metals Laboratory, VTT-MET B-131.
- (36) WALLIN, K. (1989) The effect of ductile tearing on cleavage fracture probability in fracture toughness testing, *Engng. Fracture Mech.*, **32**, 523–531.
- (37) BRÜCKNER, A. and MUNZ, D. (1984) Scatter of fracture toughness in the brittle-ductile transition region of a ferritic steel, *Advances in Probabilistic Fracture Mechanics – PVP 92*, The American Society of Mechanical Engineers, 105–111.
- (38) EHL, W., MUNZ, D., and BRÜCKNER, A. (1986) Crack extension in the ductile-brittle transition region, *Seminaire International sur L'Approche Locale de la Rupture*, Moret-sur-Loing, 233–242.
- (39) WALLIN, K. (1989) The effect of ligament size on cleavage fracture toughness, *Engng. Fracture Mech.*, **32**, 449–457.
- (40) McMEKING, R. M. and PARKS, D. M. (1979) On criteria for J-dominance of crack-tip fields in large scale yielding, *Elastic-Plastic Fracture, ASTM STP 688*, (Edited by J. D. Landes, J. A. Begley, and G. A. Clarke), ASTM, Philadelphia, pp. 175–194.
- (41) MUDRY, F., di RIENZO, F., and PINEAU, A. (1989) Numerical comparison of global and local fracture criteria in compact tension and center-crack panel specimens, *Nonlinear Fracture Mechanics: II – Elastic-Plastic Fracture, ASTM STP 995*, (Edited by J. D. Landes, A. Saxena, and J. G. Merkle), ASTM, Philadelphia, 24–39.
- (42) AMAR, E. and PINEAU, A. (1986) Application of a local approach to ductile-brittle transition in a low-alloyed steel, *Seminaire International sur L'Approche Locale de la Rupture*, Moret-sur-Loing, 221–232.
- (43) SATOH, K., TOYODA, M. and MINAMI, F. (1987) Thickness effect in fracture of steel welds, *IIFW Doc. X-1135-87*.
- (44) ANDERSON, T. L. (1989) Crack tip parameters for large scale yielding and low constraint configurations, *Int. J. Fracture*, **41**, 79–104.
- (45) IWADATE, T., TANAKA, Y., ONO, S., and WATANABE, J. (1983) An analysis of elastic-plastic fracture toughness behavior for J_{IC} measurement in the transition region, *Elastic-Plastic Fracture: Second Symposium. II – Fracture Resistance Curves and Engng App.*, *ASTM STP 803*, (Edited by C. F. Shih and J. P. Gudas), pp. II-531–II-561, ASTM, Philadelphia.
- (46) BRÜCKNER-FOIT, A., EHL, W., MUNZ, D., and TROLLENIER, B. (1990) The size effect and microstructural implications of the weakest link model, *Fatigue Fracture Engng. Mater. Structures*, **13**, 185–200.
- (47) WALLIN, K. (1989) Fracture toughness testing in the ductile-brittle transition region, *Advances in Fracture Research (Fracture 89), 7th International Conference on Fracture*, (Edited by K. Salama, K. Ravi-Chandar, D. M. R. Taplin, and P. Rama Rao) vol. 1, pp. 267–276.
- (48) BRYAN, R. H., BASS, B. R., BOLT, S. E., BRYSON, J. W., CORWIN, W. R., MERKLE, J. G., NANSTAD, R. K., and ROBINSON, G. C. (1987) Pressurized-thermal-shock test of 6-in.-thick pressure vessels PTSE-2: Investigation of Low Tearing Resistance and Warm Pressing, Oak Ridge National Laboratory NUREG/CR-4888, ORNL-6377, Oak Ridge, TN.